

Figure 7: Spectra of the symbiotic star MWC 560 as obtained with FEROS (top,  $t_{exp} = 15$  min) and shortly after with the B&C (bottom,  $t_{exp} = 30$  sec). In between, only the slit unit was moved between the corresponding two positions.

apply routinely the merging of the wavelength calibrated echelle orders into a single and complete one-dimensional spectrum as done by the FEROS on-line DRS.

The FEROS on-line DRS pipeline as installed at the ESO 1.52-m telescope is an extension to the `feros` context. The on-line DRS is initialised with a set of calibration exposures taken daily before sunset. The initialisation programme provides the DRS with all frames (e.g. extracted flatfields) and tables (e.g. order positions, dispersion coefficients) for the coming night. During the observations, each incoming spectrum is archived on tape and processed according to its descriptor information, e.g., science frames are completely reduced into a flatfielded, wavelength-calibrated, barycentric-corrected, and merged one-dimensional spectrum, which allows the observer to inspect the spectrum about 6 minutes after the shutter is closed (using one-channel CCD readout and optimum extraction). Figure 6 shows the spectra of two faint metal poor stars which have been reduced by the on-line DRS with optimum extraction.

### Observing with FEROS

The new FEROS instrument has been integrated in the existing telescope and B&C instrument environment in the ESO 1.52 control room. The user will find one additional Linux PC controlling the new

common calibration unit for B&C and FEROS and the FEROS CCD, which uses the Danish BIAS software as known from the earlier days of DFOSC at the Danish 1.54-m telescope. The B&C exposures are still defined on the nearby HP 1000 system. Both, FEROS and B&C transfer their CCD frames to the HP instrument workstation where the FEROS on-line DRS and the B&C quick-look software are running in parallel on two different workspaces.

The change between the two instruments is very simple and requires only a manual movement of the new slit unit between the two corresponding positions. Figure 7 gives a nice demonstration of the possibility to use both instruments shortly one after the other. The figure shows the H $\beta$  line of the symbiotic star MWC 560 as obtained in high spectral resolution with FEROS and in low resolution with the B&C a few minutes later after a change of the slit unit. The change between the two instruments is currently not offered to the observers but it is easy to imagine scientific programmes which could gain from this symbiosis of these two in a certain sense complementary instruments. For example, for the first time high-quality high-resolution spectrophotometric programmes could be carried out easily by combining flux-calibrated low-resolution B&C spectra with the spectral details as obtained from FEROS.

The experience from several test observing nights with FEROS at the ESO 1.52-m telescope showed that some effort is needed to reach always the maximum possible performance of FEROS in combination with the ESO 1.52-m. Particularly, it turned out that a proper focusing of the telescope on the fiber apertures is crucial to feed a maximum of light to the fibers. This is due to the use of microlenses in the focal plane which convert the slow f/15 telescope beam into a quite fast f/4.5 beam that is naturally more sensitive to defocus. Also bad seeing of more than 1.5 arcsec considerably affects the efficiency of the telescope + instrument system. Together with a bad telescope focus quickly half of the photons from the object are lost for the spectrograph.

Apart from the focus, the expected S/N for different environmental conditions is quite reliably estimated with the FEROS exposure-time calculator (ETC).

### Further Information

All information concerning the status of the instrument (e.g. the CCD upgrade) and the preparation and execution of observations with FEROS (e.g. the ETC and the User Manual) can be found on the corresponding 2p2-team homepage<sup>1</sup>. In addition, this page provides links to more pictures and reports on the installation and commissioning phases of the FEROS instrument.

### Acknowledgements

Commissioning being at the end of the 'food chain', we would like to thank here all the people actively involved in the FEROS installation and commissioning at La Silla: Our special thanks go to the 2p2-team, Wolfgang Eckert and his mechanics team, the detector group, the optics lab with Alain Gilliotte and Roberto Tighe, and Fernando Luco and the infrastructure support team.

Further big thanks go to the FEROS PI, Bernhard Wolf, and the FEROS teams in Heidelberg and Copenhagen, and the detector group in Garching. It is thanks to all their efforts that it was possible to build FEROS and to get it operational so quickly.

<sup>1</sup><http://www.la.eso.org/lasilla/Telescopes/2p2T/EIp5M/FEROS/index.html>

A.Kaufer@lsw.uni-heidelberg.de

## Monitoring of the Atmospheric Sodium above La Silla

N. AGEORGES, National University of Ireland, Galway; Physics Department, Galway, Ireland

N. HUBIN, ESO

### 1. Introduction

This work corresponds to preparatory work for the laser guide star adaptive optics system planned for the VLT at

Paranal. In this framework ESO and the National University of Ireland, Galway, are collaborating within the Training and Mobility of Researcher programme on "Laser guide star for 8m class tele-

scopes", funded by the European Commission.

In Laser Guide Star (LGS) Adaptive Optics (AO), a laser is used to excite the mesospheric (90 km altitude) sodium

(Na) layer and thereby creates an artificial star that can be used as reference for the AO wavefront sensor. The intensity of the artificial star depends strongly on the amount of Na present in the atmosphere. It has been shown that this quantity varies seasonally but also on a day-to-day basis (see e.g. Ageorges et al., 1998, and references therein). However, the only existing measurements in the southern hemisphere have been done some 20 years ago in Brazil (Clemesha et al., 1978). No information exists on the absolute amount of sodium in the atmosphere in Chile. La Silla is at a different latitude than Paranal but measurements there will be good estimators of the amount of atmospheric sodium one can expect above Paranal.

Experiences to measure the column density and details of excitation of scattering properties of sodium atoms in the atmospheric sodium layer are very important to refine the design parameters of laser and assess the power requirement.

The observations aimed at determining the absolute averaged sodium density in the atmosphere above La Silla and the night and day-to-day variations. The data were obtained during one and a half night granted DDTTC time in July 1998, on EMMI at the NTT. For this study, unreddened young bright stars of A or B type, closer than 50 pc to avoid any contamination of the spectrum by interstellar sodium, have been selected.

## 2. Observations

The minimum resolution to resolve the atmospheric sodium D lines from nearby contaminating water lines is of 50,000. This thus implied the choice of the echelle grating #14, which has a pixel size of 40 mÅ.

To get 15% error on the measure of the D<sub>1</sub> equivalent width, one would like a signal-to-noise ratio (SNR) of 1000, with:

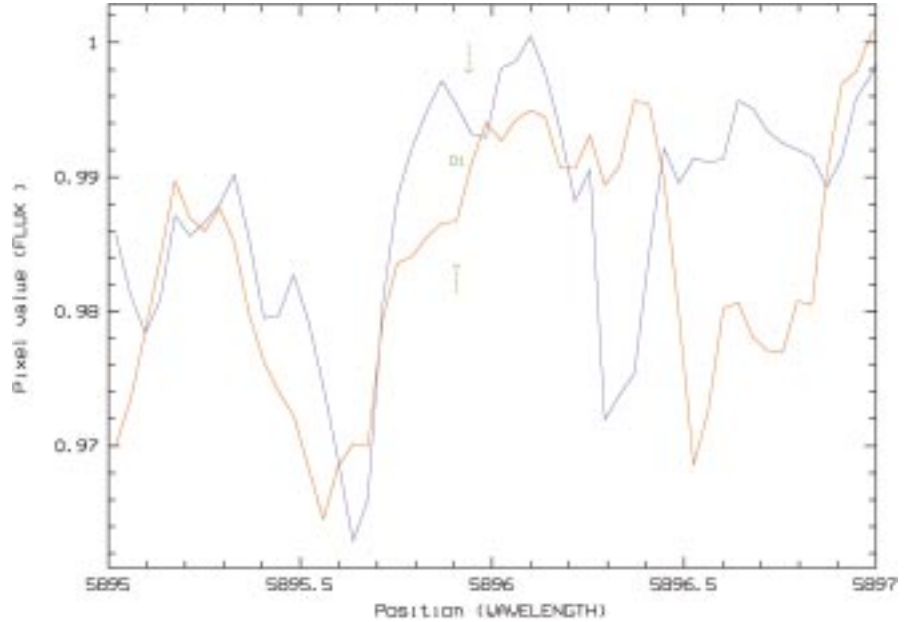


Figure 1: Spectrum of  $\theta$  Cap (blue). It is the sum of 28 spectra corresponding to 5870 seconds of integration on source. The D<sub>1</sub> line is clearly resolved at 5895.96 Å. Overplotted (in pink) is the spectrum of  $\beta$  Lib, corresponding to 2325 seconds on source.

$$SNR = \frac{DQE \times \delta\lambda \times N_{obj} \times t}{\sqrt{(DQE \times \delta\lambda \times N_{obj} \times t) + (DQE \times \delta\lambda \times N_{sky} \times t) + DN^2}} \quad (1)$$

where DQE is the detector quantum efficiency (0.65 for EMMI),  $\delta\lambda$  the width of a spectral resolution element (in Å),  $N_{obj}$  the number of photons per second per Å per spatial resolution element incident on the detector from the object,  $N_{sky}$  same as  $N_{obj}$  but for photons from the sky,  $t$  the integration time (in seconds) and  $DN$  the detector noise per resolution element. Since we are considering only bright stars ( $m_V < 6$ ), the sky contribution is negligible and will thus not be considered in this calculation.

The detector of interest is the CCD #36, which has a read-out noise of 5 electrons/pixel and a dark of 1.7 electrons/pixel/hour, so that  $DN = N \times 5 + (1.7/3600)$

$\times t$ , with  $N$  the total number of exposures. This term is however negligible since the observations are dominated by the photon noise. It is thus reasonable to approximate the signal to noise ratio by:

$$SNR \approx \sqrt{(DQE \times \delta\lambda \times N_{obj} \times t)} \quad (2)$$

The slit has been selected to have 1" width and 6.5" length on the sky, corresponding to an expected resolution of 60,000.

For EMMI at the NTT and the echelle grating used, Dekker et al. (1994) quote the arrival of 1 photon/Å/sec at 5500 Å for a  $m_V = 16.6$  star, at an airmass of 1. This number is multiplied by 57444 when observing a star with  $m_V = 4.7$ . Knowing the pixel size and the pixel scale of 0.27", this gives  $N_{obj} = 620.4$  photons/Å/sec. Taking the quantum efficiency of the detector into account, 403.3 electrons/Å/sec are arriving on the detector. Since the linearity of the detector is 50,000 ADUs, and the gain 2.2 electrons/ADU, up to  $1.1 \times 10^5$  electrons can be received without leaving the linear regime. One can thus integrate for  $\approx 273$  seconds when observing a  $m_V = 4.7$  star, without saturating the detector. To reach the desired signal-to-noise ratio, we will then have to make, e.g., 23 exposures of 4 minutes, which represents 2 hours on the source when taking the overheads into account.

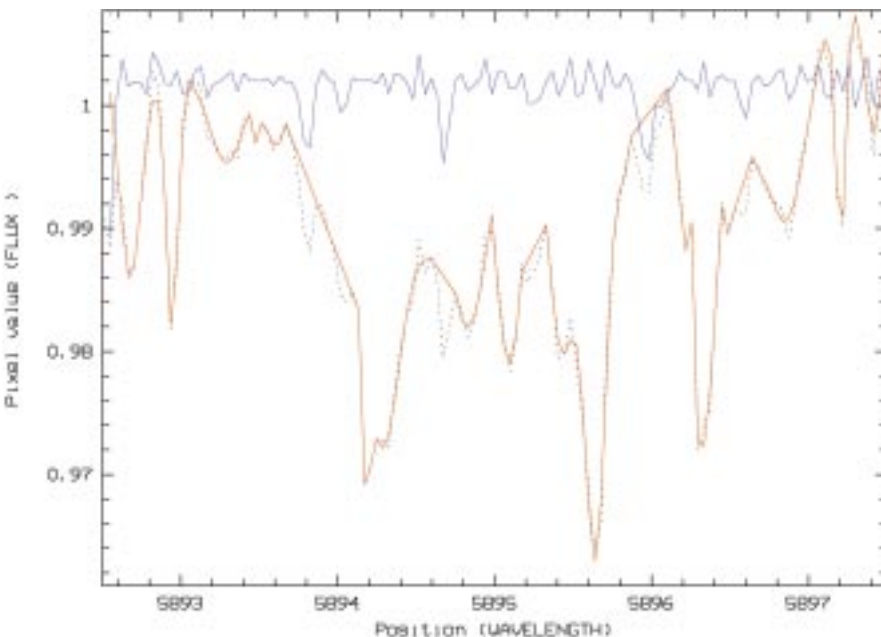


Figure 2: Spectrum  $\theta$  Cap. The dotted black line is the original spectrum, the model fitted is in pink, and the resulting spectrum is overplotted in blue (with an artificial offset of 1).

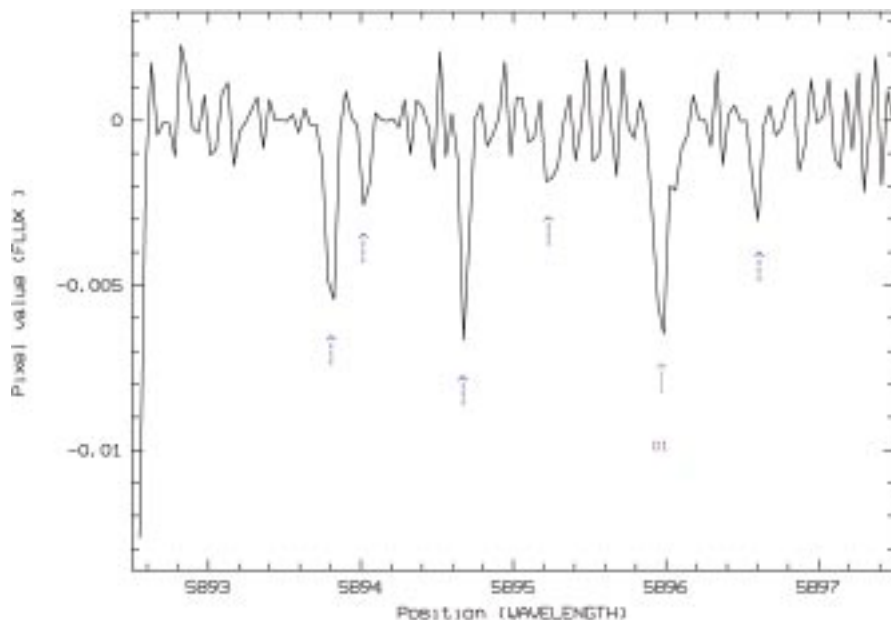


Figure 3. Final spectrum of  $\theta$  Cap, resulting from the difference between the observed spectrum and the modelled one. Blue arrows indicate lines that were not identified and are thus remaining. The pink arrow points at the atmospheric sodium  $D_1$  line, whose equivalent width is 0.5 mÅ.

### 3. Results

Only 3 sources could be observed and, unfortunately, mostly because of bad weather, one could never spend enough time on source to reach the desired signal to noise. Indeed,  $\beta$  Lib,  $\theta$  Cap and  $\iota$  Cen were observed respectively for a total of 2325, 5870 and 210 seconds on source.

Figure 1 represents spectra obtained with EMMI at the NTT. Each spectrum has been flatfielded individually, wavelength calibrated and finally coadded to the others to create this image. The data reduction has entirely been done under the echelle context of MIDAS. All further data analysis concerns only the  $\theta$  Cap data, since it has the highest integration time, i.e. the best signal on source.

Since the Moon was 80% full during the observation, strong solar lines reflected off the Moon interfere with the observed spectrum. The best illustration is visible in Figure 1 where at 5895.55 for  $\beta$  Lib and 5895.65 for  $\theta$  Cap appears a Doppler shifted solar sodium line. Most of the other lines identified in the spectrum correspond to atmospheric water contribution.

To calibrate the spectrum from the atmospheric contribution, except the mesospheric sodium, lines have been identified, fitted and suppressed. The contaminating lines to be suppressed

have been identified thanks to the table of atmospheric and solar lines (essentially from Lundström et al., 1991 and Moore et al., 1966). Calibration of future observations are planned to be done in two ways: observe a blank sky to determine the exact position of the atmospheric lines; and compare spectra of at least 2 different sources, observed the same night, to identify the lines of solar origin thanks to their relative Doppler shift. It is also expected to be able to use a code creating a synthetic atmospheric spectrum.

The lines have been geometrically fitted with Gaussians and then merged into a spectrum corresponding to our model of the data (see Fig. 2). As can be seen in Figure 3, the signal to noise of the result is dependent not only on the total integration time but also on the quality of the fitting. We derived an equivalent width of  $\approx 0.5$  mÅ at  $3.5 \sigma$ .

### 4. Discussion

Further analysis is on-going to determine the sodium column density present in the atmosphere at the time of the observation. From this information, one can derive the minimum laser power necessary to obtain a given magnitude for the laser guide star. This is one of the main information of interest in our study.

Due to the dynamic range of the CCD and the minimum exposure time needed on source to reach the requested SNR, the time resolution on the atmospheric sodium is at best 2 hours, with this type of observations. It is thus impossible to study short time-scale variations of the mesospheric sodium column density. However, this kind of study has to be pursued over at least a year period to determine the 'absolute' yearly minimum expected in the Na column density. Spectroscopic observations are thus very good for statistical studies of the atmospheric sodium.

Among the observing facilities present at La Silla, the CES, which is now fibre coupled to the 3.6-m, is the best solution in that it offers a resolution of up to 220,000. This would then allow both the Na  $D_1$  and  $D_2$  lines to be resolved from neighbouring water lines. One has thus a double check on the results.

The observations presented here also serve to refine the specifications of a portable atmospheric sodium layer monitor presently under study. This type of system could be developed for Paranal to make a site study and give some input to the VLT observing scheduler for LGS AO observations.

### 5. Acknowledgements

We would like to thank G. Mathys for his excellent advice before observing and N. Hurtado, J. Miranda and M. Pizarro for their support during all the time of the observations. Special thanks go to O. Hainaut and P. Ballester for their significant help during the data reduction.

NUIG and ESO are part of the EU TMR Network 'Laser Guide Star for 8m-class Telescopes' (contract no. FMRX-CT96-0094). NA is grateful to the EU for financial support.

### References

- Ageorges N., Hubin N., Redfern M., 1998, ESO-OSA proceedings, Sonthofen Sept. 7–11.
- Clemesha B.R., Kirchoff V.W.J.H., Simonich D.M., Takahashi H., 1978, *Geophys. Res. Let.* **5**, 873–876.
- Dekker H., D'Odorico S., Fontana A., 1994, *The Messenger* **76**, 16–20.
- Lundström I., Ardeberg A., Maurice E., Lindgren H., 1991, *A&A Suppl. Series* **91**, 199–208
- Moore C.E., Minnaert M.G.J., Houtgast J., 1966, *The Solar Spectrum 2935Å to 8770Å*.

N. Ageorges  
nancy@physics.ucg.ie